# Compressive Sensing Hardware for Analog to Information Conversion

Zora Slavik, Marc Ihle
Karlsruhe University of Applied Sciences
Fac. of Electrical Engineering and Information Technology
zora.slavik@hs-karlsruhe.de; marc.ihle@ieee.org

***Abstract*— The aim of sending an increasing amount of data in a decreasing span of time makes signal acquisition a challenging task. Unfortunately, the development of faster ADCs does not hold track with the development of faster digital signal processing hardware and therefore will become a bottling in the near future. In the recent years Compressive Sensing came up as a promising sub-Nyquist sampling method. The benefits from Compressive Sensing consist in simplified sampling tasks and a wide field of possible applications. Using the example of a single pulse as representative of an ultra wide band (UWB) signal, the information content can be uniquely defined by a set of two parameters: The amplitude and the time stamp of the incident. With Compressive Sensing these two paramters of interest can be derived from few observations. Instead of a classical AD conversion an analog-to-information conversion (A2IC) is performed. In this paper a Compressive Sensing hardware architecture called Random Signal Preintegration (RMPI) [4] was implemented with an eye to sparsity in time. It will be shown, how the RMPI architecture was implemented from the mathematical point of view and how the mathematical model was transferred to real hardware. In simulations it will be established, how the unique solution using this specific RMPI hardware can be found. The A2IC proposed in this paper does not obviate the need for ADCs, but for high sampling rates. While this work was focussed on sparse signals in the time domain, it can be shown, that the RMPI architecture covers a variety of possible applications. The implemented hardware can be applied for radio frontend architectures using the sparsity of a signal in any convenient domain. With only few modifications the hardware also can be used for searching the spectrum in Cognitive Radio applications.**

***Index Terms*— Compressive Sensing, RMPI, analog-to-information conversion, analog-to-digital conversion**

## I. Introduction

COMPRESSIVE Sensing (CS) is a sub-Nyquist sampling method, which offers a new approach to analog-to-digital conversion. Instead of acquiring signal values using equidistant time steps according to the Sampling Theorem, the signal is condensed into few values. This can be achieved with the Random Modulation Pre-Integration (RMPI) hardware architecture as proposed by [4]. Because the information obtained in a signal is traced back based on the few values, which result from the measuring process, RMPI describes an analog-to-information conversion (A2IC). The proposed A2IC method is applicable to all signals, that can be described by a finite set of parameters. This is true for signals as are used for impulse time-of-flight (ToF) measurements or ultra wide band signals, both regarded in the time domain. The finite set of parameters describing the pulse-shaped signals consists of the amplitude and the accompanying point in time, at which one pulse occurs. This paper is focussed on the hardware implementation of the RMPI architecture and the proof of concept for single-pulse signals in the time domain.

With the development of digital signal processors (DSP) of rapidly increasing speed the well-known Nyquist-Shannon sampling theorem is stretched to its limit. While processing digital data picked up speed, the interface between the analog and the digital domain still acts as a brake. This situation results from the fact, that the development of faster ADCs, which determine the highest achievable sampling rate, lags far behind the development of faster DSPs. But even if there were ADCs allowing arbitrary high sampling rates, an efficient sub-Nyquist method as CS obviates this effort and therefore reduces cost. As hinted before, many signals can be described precisely by a finite set of parameters. This implies, that actually it would be sufficient to gather only the values of the parameters to receive the information of the signal, instead of sampling a large amount of signal values, which afterwards are not needed anyway.

The theoretical approach to CS was addressed in the past years in a variety of papers. A sparse signal is

defined as a linear combination of an arbitrary small subset of a larger set of basis functions. Each sparse signal can be described by a set of parameter pairs. The first parameter depicts which basis function of the set is selected and the second parameter represents the non-zero gain used as scaling factor for the linear combination. The rationale of CS is the insight, that such a sparse signal can be reconstructed exactly from few linear measurements, as explained in [2]. The amount of required measurements strongly depends on the sparsity of the signal in the chosen domain, but not on the bandwith. E.g. if the Fourier series is used as basis functions, a sinusoidal signal is a sparse signal in the frequency domain, as it can be expressed as a single pair of parameters, indicating the frequency bin and the complex amplitude for the corresponding frequency.The sparsity restriction can be fulfilled in any arbitrary domain, in which a representation of the interesting signal exists. Fundamentals focussed on signal recovery are imparted in [13] based on image reconstruction. Also [4] emphasis on image reconstruction, but the focus lies on questions regarding the signal acquisition process. A wide overview of the state of the art is presented in [7]. For signal acquisition several measurement signals are needed, which are as incoherent as possible to the interesting sparse signal. It was shown in [13], [4] and proofed in [12], that with incoherent measurements results from the reconstruction process can be even improved compared to results obtained from measurements with coherent signals, approaching an autocorrelation strategy. Furthermore, with incoherent measurement signals significantly less measurements are needed, as deduced in [6] and [3]. While the measurement process is linear, the recovery process is solved with convex programming [13]. For recovery either a classical optimization problem can be stated, such as interior-point algorithms [13], or greedy algorithms can be used. A variety of greedy algorithms is enlisted and described in [7], while [16] compares two specific algorithms. The idea of A2I conversion using RMPI was mentioned in [4]. A closer look on the performance of Random Demodulators (RD), which is similar to the RMPI, is given in [17] based on software simulations. [7] contains an overview of possible hardware concepts for realizing CS. One of the rare CS hardware realizations is described and presented in [11].

In this paper the realized RMPI architecture will be presented. It will be explained how it can be implemented from the mathematical point of view and how the mathematical model was transferred to real hardware. The difficulties concerning the hardware realization, which arise from the mathematical model, will be explained in the paper, too. Additionally an example will be presented, how adequate measurement signals can be generated in the analog domain. It will be established by simulations, how the unique solution using this specific RMPI hardware can be found.

## II. The mathematical concept behind CS

The two most important charasteristics of a signal, CS can be applied to, are sparsity and the possibility to obtain the signal with linear combination. As mentioned above, sparsity can be fulfilled for any arbitrary domain, in which the signal of interest can be represented as a linear combination. The sparsity of a signal is defined with the number of basis functions, that are needed to represent the interesting signal. A signal composed of $s$ basis functions is $s$-sparse [3]. We define the $n$ basis vectors $\psi_k \in \mathbb{R}^{n\times 1}$, $0 \leq k < n$ to represent any of the possible input signals. Then, the columns of the square basis matrix $\mathbf{\Psi} \in \mathbb{R}^{n\times n}$ consist of the basis vectors $\psi_k$. The linear combination is conducted with the $s$-sparse vector $\mathbf{x}$, so the resulting signal vector $\mathbf{f}$ can be described with

$$\mathbf{f} = \mathbf{\Psi x} \quad . \tag{II.1}$$

Instead of performing a signal acquisition conforming the sampling theorem, the signal is correlated with $m \ll n$ measurement signals, that are represented in the $m$ rows of the measurement matrix $\mathbf{\Phi} \in \mathbb{R}^{m\times n}$.

$$\mathbf{b} = \mathbf{\Phi f} \tag{II.2}$$

Inserting (II.1) in (II.2) leads to

$$\mathbf{b} = \mathbf{\Phi\Psi x} \tag{II.3}$$

with the reconstruction matrix $\mathbf{A} = \mathbf{\Phi\Psi} \in \mathbb{R}^{m\times n}$. Because $\mathbf{b}$ contains the values, that are actually measured, the only unknown quantity is $\mathbf{x}$. If $\mathbf{A}$ was a quadratic matrix, the problem could be solved simply by inverting $\mathbf{A}$, which would result in applying the sampling theorem. But as $\mathbf{A}$ is a rectangular matrix, it cannot be simply inverted. Thus it appears, that an underdetermined system of equations with $m$ equations and $n$ unknowns is to be solved. At this point the importance of sparsity turns out, because based on this requirement a unique solution for the system of equations can be found. Due to the given sparsity it can be assumed, that the one solution out of the

amount of possible solutions is the right solution, with the most sparse $\mathbf{x}_o$. The sparsity $s$ of $\mathbf{x}_o$ is equivalent to the $\ell_0$ pseudo-norm of $\mathbf{x}$. The $\ell_0$ norm is defined as the number of elements in a vector, which differ from zero.

$$\ell_0 : \ \|x\|_0 := \{i : x_i \neq 0\} \tag{II.4}$$

Because it does not fulfill all norm axioms, the $\ell_0$ norm is referred to as pseudo-norm [5]. So sparsity is an additional information, which is used to find the optimal solution.

$$\min \|x\|_0 \text{ s.t. } \mathbf{Ax} = \mathbf{b} \tag{II.5}$$

The aim of minimizing the $\ell_0$-pseudo-norm can only be approached by brute-force methods. With further conditions limiting the solution set to a reasoable size, these methods surely can be considered. However, a more general approach would be prefarable. It was deduced in [8], that for highly sparse signals the $\ell_1$ norm

$$\ell_1 : \ \|x\|_1 = \sum_{i=1}^{n} |x_i| \tag{II.6}$$

The minimizing objective changes then into

$$\min \|x\|_1 \text{ s.t. } \mathbf{Ax} = \mathbf{b} \quad . \tag{II.7}$$

Minimizing the $\ell_1$ norm means minimizing a convex optimization problem [13], which guarantees to find a correct optimal solution, if it exists. Furthermore, with minimizing the $\ell_1$ norm classical efficient optimization algorithms such as interior-point methods can be used as well as greedy algorithms [7]. A detailed explanation of different optimization approaches inclusive of Matlab code gives [1]. Greedy algorithms are discussed in [7] and [16]. It was stated above, that the number of measurement signals should be smaller than the length of the signal vector $\mathbf{f}$, i.e. $m \ll n$. However, this poses the question about the lower bound for $m$ and how it depends on the signal's sparsity. Furthermore, the requirements for the measurement signals have to be defined. The structure of the measurement signals mainly depends on the structure of the basis signals [4]. The mutual coherence $\mu(\mathbf{\Phi}; \mathbf{\Psi})$ describes the maximal similarity, that can be found between a measurement signal $\varphi_i$ and a basis signal $\psi_j$ in the corresponding matrices [12]. $i, j$ stand for the row and column indices, respectively, for which the maximal spatial product can be reached. In other words, the mutual coherence specifies the orthogonality between the measurement matrix $\mathbf{\Phi}$ and the basis signals matrix $\mathbf{\Psi}$. Additionally, the mutual coherence is normalized to its lower bound [4], which explains the factor $\sqrt{n}$.

$$\mu(\mathbf{\Phi}, \mathbf{\Psi}) = \sqrt{n} \cdot \max_{1 \leq i,j \leq m,n} |\langle \varphi_i, \psi_j \rangle| \tag{II.8}$$

The minimal mutual coherence between two bases is according to [**?**]

$$\mu(\mathbf{\Phi}, \mathbf{\Psi}) = \frac{1}{\sqrt{n}} \tag{II.9}$$

Considering the normalizing factor, the mutual coherences lies in the range of $[1, \sqrt{n}]$. The mutual coherence has linear influence on the number $m$ of measurement signals, that are needed at least [2].

$$m \geq \mu^2(\mathbf{\Phi}, \mathbf{\Psi}) \cdot s \cdot \log(n) \tag{II.10}$$

The suggestion from (II.11) is surprising but simple. The more the measurement signals differ from the set of basis functions, the fewer measurement signals are needed. Conversely, a high similarity between the measurement signals and the basis signals turns the measurement procedure into a signal search using autocorrelations as are common in multicarrier techniques or radar applications. The reconstruction for CS is based on the search for adequate signals out of a set of $n$ basis functions. So using autocorrelations for this set-up means to calculate up to $n$ crosscorrelations, if the original signal was derived from a single basis function. This effort can be avoided by simply using incoherent measurement signals as proposed in [12]. With ultimately incoherent measurement signals the mutual incoherence becomes $\mu(\mathbf{\Phi}, \mathbf{\Psi}) = 1$. At a high probability the optimization program given in (II.7) can be solved with

$$m \geq s \cdot \log(n) \tag{II.11}$$

incoherent measurement signals [12]. For sparse signals most incoherent measurement signals are dense random sequences. There another advantage becomes obvious. In fact, the exact structure of the random measurement signals does not matter at all [4], as long as the signals are known during reconstruction. So the measurement signals have to be pseudo-random, to be more precisely. Nevertheless, this offers the possibility to simplify the measurement procedure and create a universal measurement set-up at the same time.

## III. Transfer to hardware level

The mathematical approach on CS differs from the practical implementation in one important detail. Contrary to the numeric representation of the signals

and measurements, the real signals are analog quantities. Instead of a signal vector $\mathbf{f} \in \mathbb{R}^{n\times 1}$ the observed signal $f(t)$ is continuous in time and value. Of course, this is true for all other vectors and matrices, too. Assuming, that the signal $f(t)$ is measured during the period of time $T$ the measurement process leads to

$$b_i = \frac{1}{T} \cdot \int_{\tau}^{\tau+T} \varphi_i(t) f(t)\,\mathrm{d}t \quad . \tag{III.1}$$

Obviously, a signal length $n$ and a sparsity $s$ cannot be defined for an analog signal. Instead the analog signal is mapped to the numerical model by a time grid, that is to be defined. The timeframe $T$ includes the grid points $1 \leq j \leq n$. With $\Delta t$ beeing the time distance between two points in the grid, the point $j$ means a time intervall of $j \cdot \Delta t \pm \frac{\Delta t}{2}$. The time grid poses a systematical limitation for the accuracy of the reconstruction. Applying CS allows only the reconstruction of a discretized version of the original analog signal. At this point the sampling theorem comes into play, again. The smaller $\Delta t$ is chosen, the more precise the reconstruction becomes, while $n$ and $m$ are increasing. But still the rate at which the analog signal has to be converted in the end is not affected. The only effect to the hardware is, that depending on the timeframe $T = n \cdot \Delta t$ more measurement signals are neccessary to obtain an accurate reconstruction, if $\Delta t$ is decreased.

The RMPI hardware architecture consists of pseudo-random signal generators, the multiplication of the input signal $f(t)$ with the measurement signals and the integration over time. Each measurement results in a low-frequent signal, which is then converted into the digital value $b_i$ using a standard ADC fulfilling only low demands on sampling rate. Basically, the pseudo-random signals can be provided in several ways, though the actual structure does not matter. For example, the signals can be pseudo-random $\pm 1$ sequences [4] or simply noise. Depending on the desired kind of pseudo-random signal different generators are preferable. For the RMPI hardware analog pseudo-random signal generators were designed. The generators are composed of several parallel oscillator circuits covering a wide frequency range with their resonance frequencies. At the beginning of the measurements a pulse is put on the generators' input. The resulting pseudo-random signals $\varphi_i(t),\ 1 \leq i \leq m$ correspond to the impulse responses of the generators. The measurement set-up was developed for Time-of-Flight measurements in the first place. In Time-of-Flight (ToF) measurements using unmodulated pulses, a single pulse is send out at the beginning of the measurement. So it was natural, to use this pulse in parallel as input for the generators. Additionally this had the effect, that pseudo-random signals were generated only after a pulse actually has been emitted. The impulse responses of the set of oscillator circuits were dimensioned to decay along with the timeframe $T$. This prevents following measurements to be affected from previous measurements. For general purpose the input signal can be chosen arbitrary, as long as it covers a wide frequency range. For reconstruction the transfer function of the analog circuit and the input signals are used to obtain the entries for the measurement matrix $\mathbf{\Phi}$, which represents the analog measurement signals in its rows. As hinted before, the spatial product of original signal and measurement signals becomes a multiplication followed by integration as in (III.1). Due to the large bandwidth of all signals prior to integration, it was neccessary to design the analog circuit using RF design strategies. The multiplication was realized with a multiplier IC capable of frequencies from DC to 2 GHz. To guarantee, that all multipliers would receive the same signal, the original wideband signal was fed in at one point in the center of all multipliers. To guarantee, that all multipliers would receive the same signal, the original wideband signal was fed into the printed circuit board such, that all the multipliers could be arranged around this point with equal distance and equal angles between the multipliers. Like this, all multiplier inputs obtain a signal with equal damping and phase shift regardless of the signal frequency. A construct like this was neccessary to cover the desired wide frequency range from DC to 2 GHz. Basically, the coupling problem occured for the input signal of the generators, too. But in contrary to the multiplier's input, different phase shifts and dampings due to the different conductor paths to the generators can be seen as parts of the generators. To do so, the different conductor paths must be modeled and considered, while defining the transfer functions. The integration was realized with an active integrator circuit, for which an operational amplifier capable for high frequencies was used. In Fig. (III.1) a schematic representation of the realized hardware is depicted. The ADCs are provided by a PXI system, on which the reconstruction procedure will be implemented.

## IV. Recovery using Matlab

During the reconstruction process it is presumed, that the basis functions of the input signal exist and

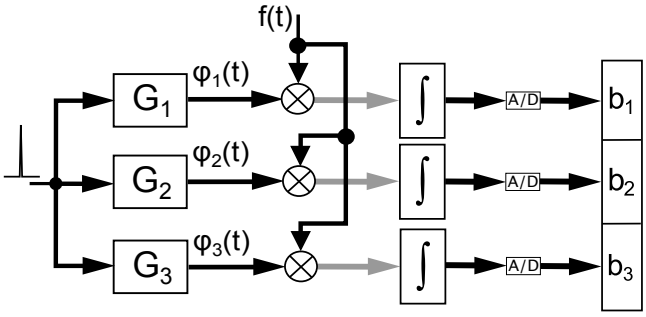


Fig. III.1. Schematic representation of the RMPI hardware architecture

are known. The evaluated setting assumed a single pulse in the time domain and therefore sparsity in the time domain. The reconstruction aim was to find the point of time in the time grid, at which the single pulse was received. So only one single parameter was considered. Therefore it was natural to choose single pulse vectors of the length $n$ with pulses occuring at $n$ different positions on the time grid. Even if the actual pulses are for example gaussian shaped and not rectangular shaped as simulated, rectangular shaped pulses as basis functions should work to obtain the paramater of the pulse location on the time grid. With this simple signal model the basis signal matrix $\mathbf{\Psi}$ was constructed as the $n \times n$ identity matrix. The pseudo-random measurement matrix $\mathbf{\Phi}$ was generated using the random signal generator implemented in Matlab. The provided signal values adhered to the standard normal distribution. For each simulated measurement process a uniformly-distributed random location on the time grid was chosen as original pulse location. The observations $\mathbf{b}$ were obtained by applying (II.2). At this point the simulation became independent from the hardware implementation. As the single pulse setting results in picking the only fitting basis vector, the reconstruction solution set was limited to $n$ possible solutions. This particularity allowed an enumerative strategy [9] as a proof of concept. The idea behind the proof of concept was, that if the optimal solution exists and the optimal solution is additionaly unique, then using all $n$ basis signals in (II.3) must provide only one valid solution. This solution uniquely explains the observation $\mathbf{b}$, that was made after applying $\mathbf{\Phi}$ to the original signal $\mathbf{f}$. Knowing this, the unique solution was identified by comparing the actual observation $\mathbf{b}$ with the result of $\mathbf{A}\mathbf{x}_j$, with $\mathbf{x}_j$ being subsequently substituted with the columns of $\mathbf{\Psi}$. The $\ell_1$ norm of the resulting error vector was taken as a quantity for the reconstruction quality.

$$\varepsilon = \|\mathbf{b} - \mathbf{A}\mathbf{x}\|_1 \tag{IV.1}$$

Using the $\ell_1$ norm was an arbitrary choice. The Euklidian norm would have worked as well as the main result remains the same. That is, that the unique solution produces an error quantity of exactly zero. But as the enumeration strategy works well for a proof of concept, it has its limits as soon as anything in the setting is changed, e.g. more than one pulse or additive noise. For a more general approach the recovery aim was formulated as an optimization problem, which can be solved with interior-point methods. Interior-point methods can be imagined as a search through a polyhedron. Its corners are different solutions for $\mathbf{x}$. The optimal solution is found following the central path, which is bounded to remain in the interior of the polyhedron [10]. To keep the search path on the central track, different methods can be used, such as the primal-dual algorithm. The rationale of the primal-dual algorithm is, that to each primal minimizing problem a dual maximizing problem exists, which can be solved instead [14]. To state the primal minimizing problem, an objective vector $\mathbf{c} \in \mathbb{R}^{n\times n}$ is introduced.

$$\text{Primal problem: } \min\{\mathbf{c}^T\mathbf{x} : \ \mathbf{A}\mathbf{x} = \mathbf{b},\ \mathbf{x} \geq \mathbf{0}\} \tag{IV.2}$$

The complementary dual problem is expressed with the dense vector $\mathbf{y} \in \mathbb{R}^{m\times 1}$ and the objective $\mathbf{b} \in \mathbb{R}^{m\times 1}$, which is known as the observation from the primal problem.

$$\text{Dual problem: } \max\{\mathbf{b}^T\mathbf{y} : \ \mathbf{A}^T\mathbf{y} \leq \mathbf{c},\ \mathbf{y} \geq \mathbf{0}\} \tag{IV.3}$$

From the duality an upper limit for the dual problem and a lower limit for the primal problem can be derived. The dual problem is limited by $\mathbf{c}^T\mathbf{x}$, while the primal problem is limited by $\mathbf{b}^T\mathbf{y}$. The difference between the limits is called the duality gap and equals zero, if the optimal solution for $\mathbf{x}$ and $\mathbf{y}$ are found [14]. During the optimization the duality gap is nonzero, of course, so the slack vector $\mathbf{s}$ is introduced to describe the gap. If the optimum is reached, $\mathbf{s}$ approximates zero.

$$\mathbf{c}^T\mathbf{x} - \mathbf{b}^T\mathbf{y} = \mathbf{x}^T\mathbf{s} \tag{IV.4}$$

In the following the matrix $\mathbf{S}$ stands for the diagonal $n \times n$ matrix, which diagonal entries are the elements of the vector $\mathbf{s}$. The same applies for the diagonal matrix $\mathbf{X}$ with only $\mathbf{x}$ substituting $\mathbf{s}$. A vector containing only ones is symbolized with $\mathbf{e}$. With the factor $\mu$ the track of the central path through the interior of the solution space is described and becomes zero, if the

optimal solution is found.

$$\mu = \frac{1}{n} \cdot \mathbf{x}^T \mathbf{s} \tag{IV.5}$$

Finally, the Karush-Kuhn-Tucker (KKT) system can be stated as follows [14]:

$$\begin{aligned} \mathbf{A}\mathbf{x} &= \mathbf{b} \\ \mathbf{A}^T\mathbf{y} + \mathbf{s} &= \mathbf{c} \\ \mathbf{X}\mathbf{S}\mathbf{e} &= \mu\mathbf{e} \\ (\mathbf{x}, \mathbf{s}) &> \mathbf{0} \end{aligned} \tag{IV.6}$$

In order to solve the optimization problem iteratively, the KKT system in (IV.6) is amended with the Newton steps $\Delta\mathbf{x}$, $\Delta\mathbf{y}$ and $\Delta\mathbf{s}$.

$$\begin{aligned} \mathbf{A}(\mathbf{x} + \Delta\mathbf{x}) &= \mathbf{b} \\ \mathbf{A}^T(\mathbf{y} + \Delta\mathbf{y}) + (\mathbf{s} + \Delta\mathbf{s}) &= \mathbf{c} \\ (\mathbf{X} + \Delta\mathbf{X})(\mathbf{S} + \Delta\mathbf{S})\mathbf{e} &= \mu\mathbf{e} \\ (\mathbf{x}, \mathbf{s}) &> \mathbf{0} \end{aligned} \tag{IV.7}$$

Solving (IV.7) for the Newton steps, the following equations are obtained:

$$\begin{aligned} \Delta\mathbf{x} &= \mathbf{S}^{-1}\mu\mathbf{e} - \mathbf{x} - \mathbf{X}\mathbf{S}^{-1}\Delta\mathbf{s} \\ \Delta\mathbf{y} &= (\mathbf{A}\mathbf{X}\mathbf{S}^{-1}\mathbf{A}^T)^{-1}(\mathbf{b} - \mathbf{A}\mathbf{S}^{-1}\mu\mathbf{e}) \\ \Delta\mathbf{s} &= -\mathbf{A}^T \cdot \Delta\mathbf{y} \end{aligned} \tag{IV.8}$$

As long as $\mu \geq \varepsilon$, new iterations are calculated, with $\varepsilon$ beeing a user defined tolerance. In the Matlab script package '$\ell_1$ magic', described and explained in [1], the primal-dual algorithm was applied to different minimizing problems in the CS context. The adequate problem statement concerning the RMPI measurement setting is also known as *basis pursuit, BP* [7], [12].

$$\min \|\mathbf{x}\|_1 \quad \text{s.t.} \quad \mathbf{A}\mathbf{x} = \mathbf{b} \tag{IV.9}$$

The recovery was analyzed in regard to reliability, depening on the number of measurement signals $m$ and noise. Alternative problem statements were also taken into account. Similar to the proof of concept in the beginning, the reconstruction error was minimized instead of $\mathbf{x}$. This method is called 'Norm Approximation' method and will be abbreviated with *NA* in the following.

$$\min_x \|\mathbf{b} - \mathbf{A}\mathbf{x}\|_1 \tag{IV.10}$$

A further possible problem statement is to minimize $\|\mathbf{x}\|$ as in (IV.9), but regarding the least square error. While making use of the known sparsity of $\mathbf{x}$, quadratic constraints (QC) are also taken into account.

$$\min \|\mathbf{x}\|_1 \quad \text{s.t.} \quad \|\mathbf{b} - \mathbf{A}\mathbf{x}\|_2 \leq \varepsilon \tag{IV.11}$$

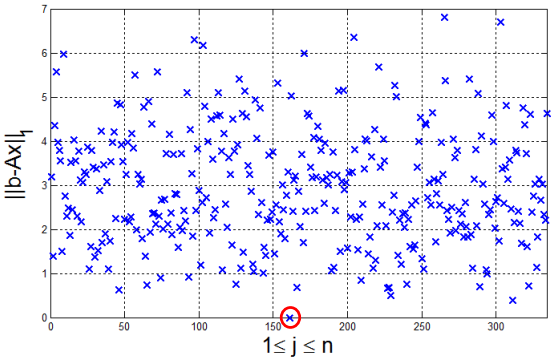


Fig. V.1. Proof of concept: The unique solution for $\mathbf{b} - \mathbf{A}\mathbf{x} = 0$.

## V. Results

For the proof of concept the CS measurement simulation ran several times and then the reconstruction was determined by using the enumarative strategy. The number of measurement signals was chosen according to (II.11). The optimal solution was found in every measurement round (1000 measurements). Besides, in every reconstruction round there was only one otimal $\mathbf{x}_o$ in the solution set, which satisfied (IV.1) exactly, i.e. the remaining error $\varepsilon = 0$. The resulting $\ell_1$ norms for a complete solution set is depicted in Fig. (V.1). While most $\ell_1$ norm values of the resulting error vectors $|\mathbf{b} - \mathbf{A}\mathbf{x}|$ show large values, there is one single $\ell_1$ norm, that equals zero (indicated by a circle). This is the unique solution of interest and it shows the uniqueness of the optimal solution. When the more general interior-point algorithm was used for reconstruction, the optimal solution was not found at a satsfying rate $m$ as proposed by $m = \log(n)$. An increasing number of measurement signals optimizes the reconstruction reliability as shown in Fig. (V.2), Fig. (V.3) and Fig. (V.4) for the three mentioned problem statements. The reliability of the reconstruction becomes optimal for a number of measurement signals of about $5 \cdot \log(n)$ of the signal length $n$ using the BP or QC problem statement. A near optimal reconstruction success rate for NA is given for $m \approx 10 \cdot \log(n)$. Taking the reconstructions into account, which produced an error on the time grid of $\pm 1 \cdot \Delta t$ and $\pm 2 \cdot \Delta t$, the success rate remains almost unchanged. Only in the range of succes rates below 20 % a slight improvement can be observed for all problems. So far, the measurements

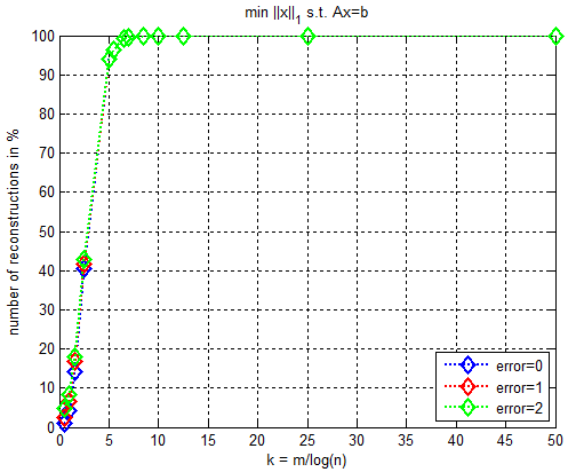


Fig. V.2. reliability depending on $k$, BP

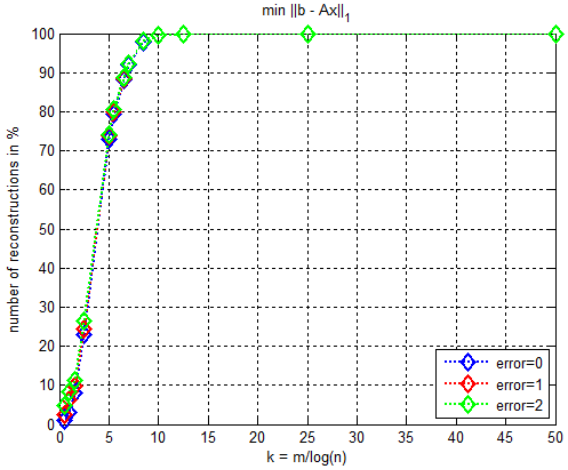


Fig. V.3. reliability depending on $k$, NA

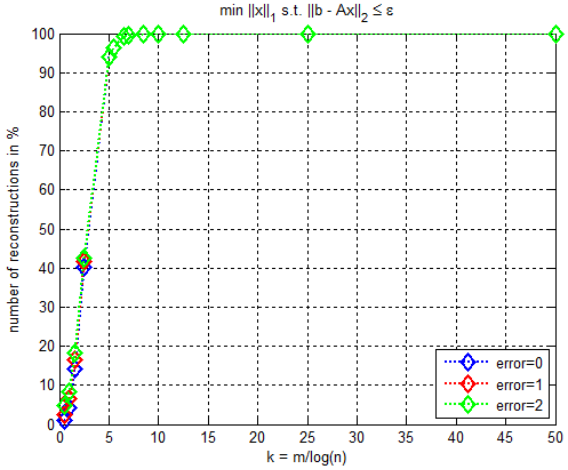


Fig. V.4. reliability depending on $k$, QC

were regarded to be noiseless. In fact, noise cannot be avoided, what poses the question, how succesfull the reconstructions can be after measuring noisy input signals. As it cannot be expected, that noisy measurements will improve a low reconstruction success rate, the effects on the reconstruction succes was only analyzed for multiples $k$ of $\log(n)$, which provided satisfying results during reconstruction. To keep it sufficiently clear, only results for $m$ beeing $10, 7$ an $5$ times $\log(n)$ were interpreted. The SNR was varied between $10$ and $40$ dB, as presented in Fig. (V.5), Fig. (V.6) and Fig. (V.7). An SNR of $40$ dB does not affect the reconstruction success. But with an SNR of $20$ dB the success for all problems and all multiples of $\log(n)$ is decreased. For low multiples of $\log(n)$ ratios the success rate drops faster, as expected. The results for BP and QC resemble each other in the course of the success rate versus SNR as well as versus the number of measurements relative to the signal length. For NA the success rate shows a smoother decay for a decreasing SNR, but it starts at a lower level compared to BP and QC, at least for the given range of $m$.

## VI. Discussion

The simulation results concerning successfull reconstructions implicate a similar performance for BP and the $\ell_1$ norm minimization with quadratic constraints. Both methods become highly reliable at a number of measurement signals, that is $5 \cdot \log(n)$. BP was implicitly recommended for the RMPI architecture in [12]. Though minimizing the $\ell_1$ norm of the remaining error works well for the proof of concept, where an enumerative reconstruction strategy was chosen, it cannot be recommanded for the RMPI structure. For a reliable performance for $m$ a double percentage on the signal length is needed compared to BP or QC. This would pose an effort on the hardware design and dimension, that can be avoided otherwise. Taking time errors of $\pm 1 \cdot \Delta t$ and $\pm 2 \cdot \Delta t$ into account, no significant improvements on reliability including these tolerances can be observed. Allowing some tolerance for the location on the time grid, even if it was acceptable for an application, will not make a change on the general results. The conclusion is, that if the optimal solution is not found, the calculated result lies far from the original parameters. More important is, that it was not possible to find the optimal solution with only $m = \log(n)$ measurement sequences as proposed in [4] and [12]. The reason can be seen in an insufficient incoherence between the measurement

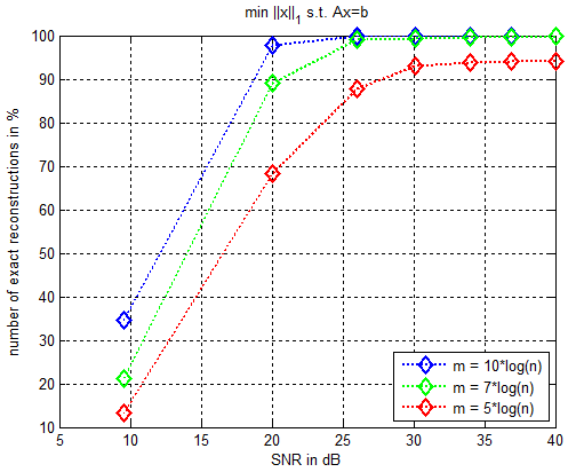


Fig. V.5. reliability depending on SNR, BP

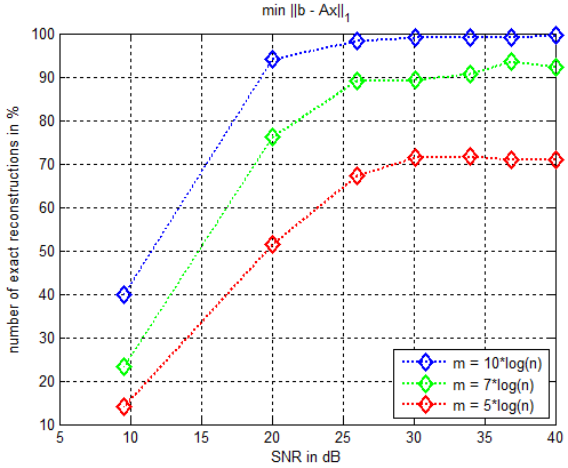


Fig. V.6. reliability depending on SNR, NA

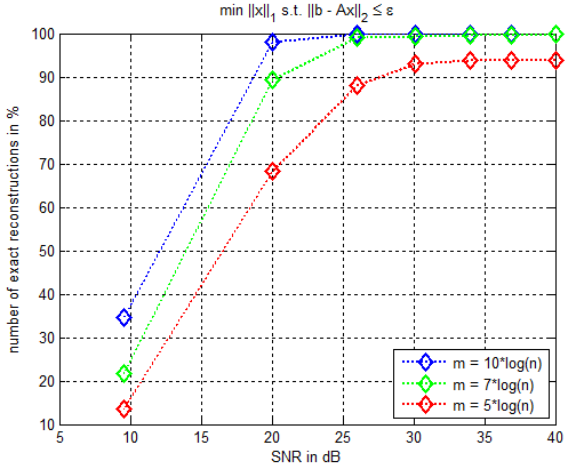


Fig. V.7. reliability depending on SNR, QC

signals and the basis functions. Improving the incoherence meaning optimizing the pseudo-random signal generation therefore could increase the reliability of the reconstruction for a less number of measurement signals. On hardware level the reliability can be improved by increasing the number of measurements. In order to do this, either more pseudo-random signal generators could be connected in parallel or the measurement signal is sent out several times, while the pseudo-random generators are slightly modified. The second alternative is especially interesting for ToF measurements, because the transmitted signal is well-known and the timing is not a critical parameter. But to receive an unknown UWB signal a sophisticated synchronisation routine would be neccessary. Additionally, temporal successive measurements would decrease the information transmission rate and therefore lowering the gain of A2IC. On the other hand, the proof of concept showed, that the unique optimal solution for $m = \log(n)$ measurement signals exits. So another promising and preferable approach is to either optimize the starting point, which is neccessary for interior-point algorithms, or to use greedy algorithms [7], [16], which are designed especially for sparse signal recovery. The noisy simulations demonstrate, that the RMPI architecture is robust to a moderate level of noise. The effect of noise to the signal depends mainly on the number of measurement signals. Increasing m leads to a more robust reconstruction success. While for $m$ beeing $5 \cdot \log(n)$ the success rate in recovery for BP and QC is not affected (NA: $10 \cdot \log(n)$), for lower $m$ the success rate drops rapidly.

## VII. Conclusion

The RMPI CS hardware can be used in an almost universal way. While the actual hardware remains unchanged, the software sided reconstruction can be modified according to the signal particularities. This qualifies the measurement frontend to be used for A2IC in different applications, such as SDR and SAR [18]. Another application, for which the hardware can be used with only slight modifications, is searching the spectrum for Cognitive Radio [15]. The sparsity is then defined as a change in spectrum allocation. Instead of random modulation, the received signal passes several lowpass filters in parallel, with each having a different cutoff frequency. In addition to low pass filters, bandpass and band rejection filters can be used. The cutoff frequencies are chosen pseudo-randomly analog to the measurement signals in the

time domain. The wide range of applications requiering only few modifications motivates to design measurement hardware on a modular basis. So Compressive Sensing and especially the RMPI hardware remains a field with many interesting research aspects.

## REFERENCES


[1] E. Candès and J. Romberg, "$\ell_1$-magic: Recovery of sparse signals via convex programming," Caltech, Tech. Rep., October 2005.

[2] E. Candès, J. Romberg, and T. Tao, "Robust uncertainity principles: Exact signal reconstruction from highly incomplete frequency information," *IEEE Transactions on Information Theory*, vol. 52, no. 2, 2006.

[3] E. J. Candès and J. Romberg, "Sparsity and incoherence in compressive sampling," *Inverse Problems*, vol. 23, no. 3, 2007.

[4] E. J. Candès and M. B. Wakin, "An introduction to compressive sampling. a sensing/sampling paradigm that goes against the common knowledge in data aquisition," *IEEE Signal Processing Magazine*, vol. 25, no. 21, 2008.

[5] M. A. Davenport, M. F. Duarte, Y. C. Eldar, and G. Kutyniok, "Introduction to compressed sensing," in *Compressed Sensing. Theory and Application*, Y. C. Eldar and G. Kutyniok, Eds. New York: Cambridge University Press, 2012, pp. 1–64.

[6] D. L. Donoho and X. Huo, "Uncertainty principles and ideal atomic decomposition," *IEEE Transactions on Information Theory*, vol. 47, no. 7, 2001.

[7] M. F. Duarte and Y. C. Eldar, "Structured compressed sensing: From theory to applications," *IEEE Transactions on Signal Processing*, vol. 59, no. 9, 2011.

[8] G. Fung and O. L. Mangasarian, "Equivalence of minimal $\ell_0$- and $\ell_p$-norm solutions of linear equalities, inequalities and linear programs for sufficiently small p." *J. Optimization Theory and Applications*, vol. 151, no. 1, pp. 1–10, 2011. [Online]. Available: http://dblp.uni-trier.de/db/journals/jota/jota151.html#FungM11

[9] B. Korte and J. Vygen, *Combinatorial Optimization. Theory and Algorithms*. Berlin Heidelberg: Springer, 2012.

[10] A. Levitin, *Introduction to the Design and Analysis of Algorithms*. Edinburgh: Pearson Education Limited, 2012.

[11] M. Mishali, Y. C. Eldar, O. Dounaevsky, and E. Shoshan, "Xampling: Analog to digital at sub-nyquist rates," *IET Circuits, Devices & Systems*, vol. 5, no. 1, pp. 8–20, 2011.

[12] J. Romberg, "Compressive sampling via random convolution," *PAMM*, vol. 7, no. 1, pp. 2 010 011–2 010 012, 2007. [Online]. Available: http://dx.doi.org/10.1002/pamm.200700036

[13] J. Romberg, "Imaging via compressive sampling," *IEEE Signal Processing Magazine*, vol. 25, no. 21, 2008.

[14] T. Roos, Cornelis ans Terlaky and J.-P. Vial, *Interior Point Methods for Linear Optimization*. New York: Springer, 2005.

[15] C. S. Seelamantula, "A generalized sampling method for finite-rate-of-innovation-signal reconstruction," *IEEE Signal Processing Letters*, vol. 15, pp. 813–816, 2008.

[16] J. A. Tropp, "Greed is good: algorithmic results for sparse approximation," *IEEE Transactions on Information Theory*, vol. 50, no. 10, pp. 2231–2242, 2004.

[17] J. A. Tropp, J. N. Laska, M. F. Duarte, J. K. Romberg, and R. G. Baraniuk, "Beyond nyquist: efficient sampling of sparse bandlimited signals," *IEEE Transactions on Information Theory*, vol. 56, no. 1, pp. 520–544, 2010.

[18] D. Xu, R. Tongret, Y. F. Zheng, and R. L. Ewing, "Wavelet-modulated pulse for compressive sensing in sar," *Aerospace and Electronics Conference (NAECON), Proceedings of the IEEE 2010 National*, 2010.